Multiphase Equilibria in Solutions of Polydisperse Homopolymers. 4. Three-Phase and Four-Phase Separations in Quaternary Systems†

Karel Šolc* and Kevin Battjes

Michigan Molecular Institute, Midland, Michigan 48640. *Received February 20, 1984*

ABSTRACT: Criteria and the mechanism for the four-phase separation in quaternary systems solvent–polydisperse polymer are established. Multiple critical points act as roots of multiphase regions. Thus, a critical point diagram displaying multiple critical points in the global space of all quaternary systems can serve as a basis for classification of their phase behavior. For instance, four-phase equilibria are potentially possible only in systems mapping beyond the quadruple critical line. A four-phase region is invariably tied to the existence of multiple three-phase regions. For instance, in systems with $d\chi/dT < 0$, two seemingly independent three-phase regions, T_1 and T_3, grow closer with decreasing temperature, form a linear contact, and T_3 penetrates into T_1, thus creating the four-phase tetrahedron with four surrounding three-phase regions. Eventually T_3 is absorbed by T_1; at this point the complex phase diagram degenerates into a single three-phase region that evolves then normally.

1. Introduction

There is little known about multiphase equilibria in solutions of polydisperse polymers. It is not a subject which would come evidently to one's mind; after all, with all polymer molecules chemically identical and differing only by their chain lengths, there does not seem to be much incentive for extensive phase separations. Yet, thermodynamically, each polymer species acts as a separate component. It is well-known that ternary and other systems can display three-phase separations,[1-7] and four-phase equilibria have been predicted for some complex systems.[5] One cannot avoid the following question (raised on one occasion by Masao Doi): Is there any limit to the number of possible phases in such systems, provided that the polymer component characteristics and the mixture compositions are properly chosen?

These circumstances led us to the examination of criteria for multiple critical points that act as roots of multiphase regions,[8] and to a detailed study of quaternary systems that are still simple enough to allow some reasonable graphical representation of phase diagrams in the limited three-dimensional space we can perceive. In our previous paper,[7] we formulated the principles governing three-phase separations in quaternary systems and examined the simplest case where only one of the constituent ternary systems also exhibited a three-phase region. Keeping the same restriction to ensure that all important features of the phase diagram stay within the physically real tetrahedron of compositions, we extend here our previous study to four-phase systems. In addition, it is shown that critical point diagrams constructed in the global space of all possible quaternary systems provide a convenient basis for classification of such systems in regard to their phase behavior.

Throughout the paper it is assumed that polymer solutions follow the Flory–Huggins thermodynamics[9] with a concentration-independent interaction parameter χ.

2. Multiple Critical Points in Quaternary Systems

Multiple critical points arise as nontrival multiple roots of phase equilibrium equations that happen to be located at the critical concentration and temperature. The highest multiplicity a critical point may attain in an s-component system is $2s - 3$.[8] Thus, a quaternary system can possess critical points of multiplicities m where $1 \leq m \leq 5$. The criteria for such points can be expressed by a succession of equations[8]

$$r_z(1 - \phi)^2 = r_w{}^2\phi^2 \tag{1}$$

$$3r_z + 2r_z{}^{1/2} - r_{z+1} = 0 \tag{2}$$

$$r_z(10r_{z+1} - 15r_z + 6) - r_{z+2}r_{z+1} = 0 \tag{3}$$

$$r_z[5r_{z+1}(3r_{z+2} + 2r_{z+1}) - 105r_z(r_{z+1} - r_z) + 12(r_{z+1} - 3r_z)] - r_{z+3}r_{z+2}r_{z+1} = 0 \tag{4}$$

$$r_z[7r_{z+2}r_{z+1}(3r_{z+3} + 5r_{z+1} - 30r_z) - 35r_z(8r_{z+1}{}^2 - 36r_{z+1}r_z + 27r_z{}^2) + 120r_z] - r_{z+4}r_{z+3}r_{z+2}r_{z+1} = 0 \tag{5}$$

where r_w, r_z, r_{z+1}, ... are the weight, z, $z + 1$, and higher averages of the chain length r, and ϕ is the total volume fraction of the polymer at the critical point. Equation 1 is recognized as the definition of the critical point concentration.[10] A polymer mixture satisfying eq 2 possesses a heterogeneous double critical point. A triple critical point mixture is determined by eq 2 and 3. Generally, a polymer mixture with a critical point of multiplicity m has to satisfy the set of equations from (2) to (m), with eq 1 specifying the critical concentration.[8]

Equations 1–5 are general and, as such, they do not offer much physical insight; we need to follow their fate within some space of physical variables. Convenient for this purpose is the triangular diagram representing the composition space $\mathbf{w}$ of weight fractions w_1, w_2, w_3, $\sum w_i = 1$, of the three polymeric components with chain lengths $r_1 < r_2 < r_3$. Although such a diagram cannot comprise all the information about the state variables (e.g., the solvent content is ignored), it enables a succinct display of most features crucial for multiphase equilibria.[7]

A prominent curve in such diagrams for quaternary multiphase systems is the HDPP line, the locus of polymer mixtures with heterogeneous double plait (critical) points. It separates mixtures with unstable and (meta)stable critical points from each other and plays an important role in three-phase separations. It has been proved that the HDPP line cannot exist as an isolated loop located entirely within the triangle of polymer compositions.[7] Hence, it has to enter and exit the triangle through one or more of its three sides, which represent in fact three ternary systems (of the type solvent + a binary polymer), constituting the given quaternary system. This means that a quaternary system cannot separate into three or four phases unless at least one of its constituent ternary systems displays three-phase behavior as well. Evidently, most prone in this respect is the ternary system solvent–polymer 1–

† This paper is dedicated to Dr. Ronald Koningsveld on the occasion of his 60th birthday.

0024-9297/85/2218-0220$01.50/0

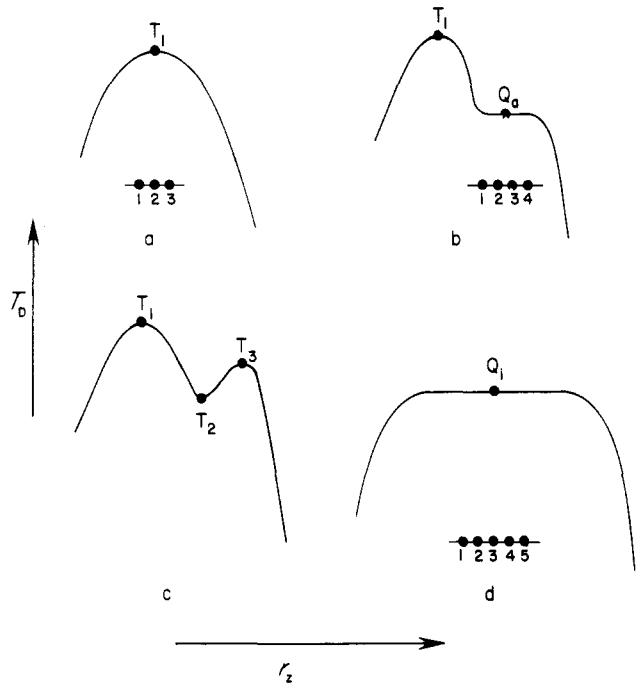

Figure 1. Multiple critical points appearing in the w-space as special points of the HDPP line. Four different quaternary systems are displayed. Coordinates: Critical temperature T_D vs. the z-average molecular weight r_z of the mixture with a heterogeneous double critical point. Critical point notation: T, triple; Q_a, quadruple; Q_i, quintuple. Dots represent single critical points whose overlapping collection defines the multiple critical point. (Reprinted from ref 8.)

polymer 3 with the highest ratio of chain lengths r_3/r_1. [Recall that the condition for three-phase separation in such a system is $r_3/r_1 \geq \rho(r_1)$ where $\rho(r)$ is a function decreasing from $\rho(1) \approx 15.645$ to $\rho(r \to \infty) \approx 9.899$.[1,6]] The HDPP line is thus always anchored by both ends to the 1–3 axis of the triangle and penetrates into its interior. Furthermore, since the critical value of χ at the HDPP line, χ_D, diminishes as one moves inward along either one of its branches, χ_D has to assume at least one minimum,[7] say at the point T. For systems with an upper critical temperature ($d\chi/dT < 0$), this would correspond to a maximum in temperature; hereafter we shall follow this sign convention. The polymer mixture of composition w_T thus possesses a double point of the HDPP line, i.e., a triple critical (or tricritical[11]) point, and satisfies eq 2 and 3.[8]

If present, critical points of higher multiplicities are also located on the HDPP line at some of its geometrically significant points. They are best viewed in the unfolded projection of the HDPP line in coordinates double critical temperature T_D vs. r_z average of the polymer mixture. (The latter variable can serve as a yardstick since it changes monotonously along the HDPP line.) For a three-phase system with one triple critical point the HDPP line is projected simply as a curve with a single maximum T_1 (see Figure 1a). Note that a small perturbation of chain lengths r_i may shift the maximum but will not remove it; physically this means that such systems will be quite common, as predicted earlier.[11-13] A large change in r_i's may lead to the formation of a shoulder and eventually of a point of inflection Q_a with a horizontal slope (Figure 1b). As a triple point of the HDPP line, such a point is equivalent to a quadruple critical point. It is apparent that the existence of Q_a on the line requires a delicate balance of parameters affecting the thermodynamic equilibrium, and a small perturbation of even one of them usually leads to the disappearance of Q_a. Indeed, it is a "lucky accident", as Griffiths says,[11] if one happens to choose the set of r_i's so as to achieve the pattern of Figure 1b. A further perturbation will usually cause splitting of the point of inflection into a pair of extrema, a maximum and a minimum, that physically correspond to a new pair of triple critical points, a stable T_3 and an unstable T_2 (cf. Figure 1c). Finally, on a very rare occasion (another "lucky accident") the three extrema T_1, T_2, and T_3 merge to a single flat maximum Q_i (Figure 1d). This point arises as an overlap of three triple critical points and is equivalent to a quintuple critical point. The common occurrence of triple critical points (patterns a and c), in contrast to rare cases with quadruple and quintuple critical points (patterns b and d), in quaternary systems has to do with the number of degrees of freedom various critical points enjoy;[8] this distinction will become more evident as we discuss critical point diagrams.

Not only is the interpretation of multiple critical points as special points of the HDPP line more telling than the abstract criteria (3)–(5), it also provides an equivalent set of conditions that is easier to handle. The argument leading to T_D vs. r_z plots of Figure 1 suggests it should be possible to recast the criteria in terms of r_z alone. Indeed, for ternary polymer mixtures a higher average is related to the two immediately lower averages as

$$r_{z+i} = R - \frac{P}{r_{z+i-1}} + \frac{T}{r_{z+i-1}r_{z+i-2}} \tag{6}$$

where

$$R = r_1 + r_2 + r_3, \qquad P = r_1r_2 + r_1r_3 + r_2r_3, \qquad T = r_1r_2r_3 \tag{7}$$

With r_{z+2} from eq 6 and r_{z+1} from eq 2, the condition (3) for a triple critical point then takes the form

$$Rr_z(3r_z + 2r_z^{1/2}) - Pr_z + T - r_z^2(15r_z + 20r_z^{1/2} + 6) = 0 \tag{8}$$

Quadruple and quintuple critical point criteria are now obtained by requesting that also the first and second derivatives of eq 8 with respect to r_z be equal to zero

$$3R(2r_z + r_z^{1/2}) - P - r_z(45r_z + 50r_z^{1/2} + 12) = 0 \tag{9}$$

$$R(2 + \tfrac{1}{2}r_z^{-1/2}) - 30r_z - 25r_z^{1/2} - 4 = 0 \tag{10}$$

The equivalence of equation sets 3–5 and 8–10 can be rigorously proved. The advantages of the latter one are obvious: it is much simpler, containing only three constants R, P, and T fully characterizing the system components, and a single variable r_z sensitive to the composition of the polymer mixture.

3. Critical Point Diagrams and Classification of Quaternary Systems

One would often like to know the maximum number of phases and the types of critical points that can appear in a given system. This information is conveniently presented in the form of a critical point diagram. Here it will be advantageous to characterize the system by r_1, and the ratios $\alpha \equiv r_2/r_1$ and $\beta \equiv r_3/r_2$ ($\alpha > 1$, $\beta > 1$); it is anticipated that the diagram patterns, plotted in α vs. β coordinates for a fixed r_1, will converge in the high polymer limit ($r_1 \to \infty$) to some limiting form.

Also introduced can be reduced parameters

$$R^* \equiv R/r_1 = 1 + \alpha + \alpha\beta,$$
$$P^* \equiv P/r_1^2 = \alpha(1 + \beta + \alpha\beta), \tag{11}$$
$$T^* \equiv T/r_1^3 = \alpha^2\beta, \qquad r_z^* \equiv r_z/r_1$$

Equations 8–10 then take the form

$$R^*r_z^*[3r_z^* + 2(r_z^*/r_1)^{1/2}] - P^*r_z^* + T^* - r_z^{*2}[15r_z^* + 20(r_z^*/r_1)^{1/2} + (6/r_1)] = 0 \quad (12)$$

$$3R^*[2r_z^* + (r_z^*/r_1)^{1/2}] - P^* - r_z^*[45r_z^* + 50(r_z^*/r_1)^{1/2} + (12/r_1)] = 0 \quad (13)$$

$$R^*(4r_z^{*1/2} + r_1^{-1/2}) - 2r_z^{*1/2}[30r_z^* + 25(r_z^*/r_1)^{1/2} + (4/r_1)] = 0 \quad (14)$$

Note that the three reduced parameters R^*, P^*, and T^* are no longer independent since

$$T^* = P^* - R^* + 1 \quad (15)$$

Each of the above sets of parameters (r_1,r_2,r_3; r_1,α,β; R,P,T; and r_1,R^*,P^*) can be easily converted into any other, and it is strictly the matter of convenience which one is used for what purpose.

3.1. High Polymer Limit. From the practical point of view, most interesting is the limit for $r_1 \to \infty$ corresponding to the behavior of truly high polymers. Also, the relations here become simple and can be tackled to some extent analytically, which contributes to better comprehension of this problem. In place of eq 12–14 we have now

$$3R^*r_z^{*2} - P^*r_z^* + T^* - 15r_z^{*3} = 0 \quad (16)$$

$$6R^*r_z^* - P^* - 45r_z^{*2} = 0 \quad (17)$$

$$R^* - 15r_z^* = 0 \quad (18)$$

From the previous analysis of multiple critical points[8] it follows that at fixed r_1, quadruple critical points Q_a have just one degree of freedom. In a two-dimensional plot of α vs. β (or R^* vs. P^*), the locus of such points thus should be a curve. Indeed, this is confirmed by eq 16 and 17, which are linear in R^* and P^* (with T^* substituted from eq 15). They are easily solved, yielding the locus of quadruple critical points with r_z^* as its parameter. The result is plotted in Figure 2 (curve Q_a) in coordinates α vs. β. The locus forms two branches, behaving as asymptotes for $\alpha \to \infty$ and $\beta \to \infty$, and joined in a cusp Q_i that corresponds to a quintuple critical point. Some features of this line can be examined analytically. For instance, eq 16 and 17 can be also solved for r_z^* with the result

$$r_z^* = [R^* \pm (R^{*2} - 5P^*)^{1/2}]/15 \quad (19)$$

$$r_z^* = [P^* \pm (P^{*2} - 9R^*T^*)^{1/2}]/3R^* \quad (20)$$

Real r_z^* thus requires that

$$5P^*/R^{*2} \le 1, \qquad 9R^*T^*/P^{*2} \le 1 \quad (21)$$

Equality signs evidently specify the cusp point of the quadruple line where its parameter r_z^* takes the value

$$r_z^* = R^*/15 = P^*/(3R^*) \quad (22)$$

This is the above-mentioned quintuple critical point (cf. eq 18), and the condition for it can be recast in terms of a single parameter as

$$R^{*3} - 45R^{*2} + 225R^* - 225 = 0 \quad (23)$$

The physically acceptable solution ($R^* > 3$, $P^* > 3$, $T^* > 1$) of eq 23 characterizing this unique point is $R^* \approx 39.440$, $P^* \approx 311.10$, $T^* \approx 272.66$, $r_z^* \approx 2.6293$, $\alpha \approx 9.3840$, $\beta \approx 3.0963$.

A similar self-contained relation for the quadruple line is obtained by substituting r_z^* of eq 19 into criterion (16) with the result

$$(225T^* + 2R^{*3} - 15P^*R^*)^2 - 4(R^{*2} - 5P^*)^3 = 0 \quad (24)$$

From here, the slope of the quadruple line at the cusp point is $d\alpha/d\beta \approx 1.292$. Also evaluated can be the two asymptotes. The results are summarized in Table I. For

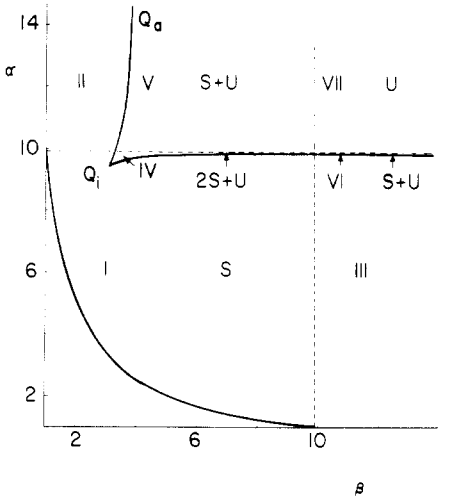

Figure 2. Critical point diagram for quaternary systems in the high-polymer limit, $r_1 \to \infty$: coordinates α and β specify the chain-length ratios r_2/r_1 and r_3/r_2, respectively; Q_a, quadruple critical line; Q_i, quintuple critical system; the hyperbolic line separates two-phase systems (below) from multiphase ones (above). Areas I–VII delineate multiphase systems with different phase diagram patterns, and different types of physically real triple critical points as indicated by letters [S, (meta)stable; U, unstable; no letter, none present].

$\beta \to \infty$ and α finite, both P^* and R^* grow linearly with β (cf. eq 11) so that P^*/R^{*2} converges to zero while $R^*T^*/P^{*2} \to 1/12$. Also r_z^* approaches from above a limit of $\approx$1.816; this is the minimum r_z^* that could ever show a quadruple critical point, if and only if simultaneously $\beta \to \infty$ and $\alpha \approx 9.899$. (Note that the same value of α is required for a triple critical point in ternary systems.) On the other hand, for $\alpha \to \infty$ and β finite, P^* grows like α^2 while R^* stays linear; thus, the ratio P^*/R^{*2} approaches 3/20, R^*T^*/P^{*2} converges to zero and r_z^* diverges like $\approx 0.544\alpha$.

In the course of the quadruple line, the positive fractions of eq 21 thus exhaust their entire allowed ranges but, reaching their maxima at the cusp Q_i, neither one of them is a suitable "yardstick" for this line. The parameter r_z^*, on the other hand, changes monotonously and defines uniquely the position of any of its points.

The existence of a quaternary system with a quadruple critical point is very rare, requiring a specific value of α (in the range $9.384 < \alpha < 9.899$) for a chosen $\beta > 3.096$, or a specific value of β ($3.096 < \beta < 4.442$) for a chosen $\alpha > 9.384$. Only then the HDPP line will be of the type displayed in Figure 1b, and one particular polymer mixture of the composition specified by the respective parameter of the line r_z^*, and by $r_{z+1}^* = 3r_z^*$ (cf. eq 2), will possess a quadruple critical point at the polymer concentration ϕ given by eq 1, and the interaction parameter (i.e., temperature) given by the spinodal condition. The quintuple critical point is even more restricted in having predetermined values of both α and β.

It is not surprising that each branch of the quadruple line is limited to relatively narrow ranges of variables α or β; after all, in ternary systems, a triple critical point appears only in systems with one particular value of the ratio r_2/r_1. Somewhat unexpected, however, are low values of β ($\approx$3.1–4.44) required for the vertical branch of quadruple line. In fact, even α values required for finite β in the horizontal branch are lower than the ratio $\approx$9.899 necessary for three-phase separation in ternary systems. Thus, one has to conclude that the appearance of quadruple and quintuple critical points in quaternary systems, accompanied by development of a second three-phase and/or a four-phase region around them, is brought on

Table I
Some Characteristics of the Quadruple Critical Line in the Limit for $r_1 \to \infty$

	α	β	r_z^*	P^*	R^*	P^*/R^{*2}	R^*T^*/P^{*2}
horizontal asymptote	$5 + 24^{1/2} \approx 9.899$	∞	$1 + (2/3)^{1/2} \approx 1.816$	$\alpha(1 + \alpha)\beta$	$\alpha\beta$	0	1/12
quintuple critical point	9.384	3.096	2.629	311.10	39.440	1/5	1/9
vertical asymptote	∞	$(7 + 40^{1/2})/3 \approx 4.442$	$(5 + 10^{1/2})\alpha/15 \approx 0.544\alpha$	$\beta\alpha^2$	$(1 + \beta)\alpha$	3/20	0

more easily than the generation of double and triple critical points with three-phase regions in ternary systems (judging by chain-length ratios of successive components). Since a similar behavior is observed for hexuple and heptuple critical points in five-component mixtures,[14] this phenomenon seems to be quite general, indicating that multiple critical points in polydisperse homopolymer solutions arise more easily than originally expected. Specifically, the presence of a $(2s - 3)$-multiple critical point in an s-component solution ($s > 3$) requires the overall ratio r_{s-1}/r_1 to be substantially smaller than $\approx 10^{s-2}$.

In addition to depicting the quadruple line and the quintuple critical point, the diagram of Figure 2 also contains other information. As mentioned above, a quaternary system can separate into three or four phases only if the ternary system solvent–polymer 1–polymer 3 possesses a three-phase region as well. The criterion for this to happen is $r_3/r_1 = \alpha\beta \geq 9.899$, and it is projected into the diagram of Figure 2 as a hyperbolic line, separating systems with exclusively two-phase equilibria and single critical points from systems showing also higher critical points and multiphase equilibria.[8]

Each system beyond the hyperbolic boundary contains an HDPP line, i.e., an infinite number of heterogeneous double critical points. No such blank statement can be made about triple critical points that, having one less degree of freedom,[8] exist only as isolated points. Systems located between the hyperbolic boundary and the quadruple line contain one thermodynamically stable triple critical point (Figure 1a), while system beyond the quadruple line possess two (meta)stable and one unstable triple critical points (projected as two maxima and a minimum of the HDPP line in Figure 1c). In either one of those cases, however, the HDPP line may protrude beyond the triangle axes 1–2 and/or 2–3, and some triple point(s) may become physically not real, being located outside the triangle of physically real polymer compositions.

The permitted phase diagram types can be determined by considering the following facts: (i) Critical temperature along the HDPP line grows when advancing from 1–3 axis inward, but diminishes when moving from 1–2 or 2–3 axes inward; the proof of this claim is found in Appendix 1. (ii) A quadruple critical point cannot be located on (nor beyond for reasons of continuity) any of the binary polymer axes; thus, the unstable triple critical point, if present, has to be contained within the triangle of compositions.

Hence, seven possible patterns of the HDPP line can be distinguished (see Figures 3–5), corresponding to seven types of multiphase quaternary systems delineated in the α–β plane of Figure 2 by the hyperbolic and cusp boundaries, and by the lines $\alpha \approx 9.899$ and $\beta \approx 9.899$ (marking the onset of three-phase equilibria in the respective ternary systems). Letters in Figure 2 denote the physically real (meta)stable (S) and unstable (U) triple critical points present in each type of system. Note that the pattern VI is very rare, being restricted to the narrow area for $\beta >$ 9.899 between the horizontal cusp line and its asymptote, and for $\beta \to \infty$ it cannot exist at all. On the other hand, the symmetrical pattern V can well appear even if $\alpha \to \infty$.

As long as the quaternary system possesses just one triple critical point (types I–III in Figure 3), phase equilibria are trivial. The case I has been analyzed in detail

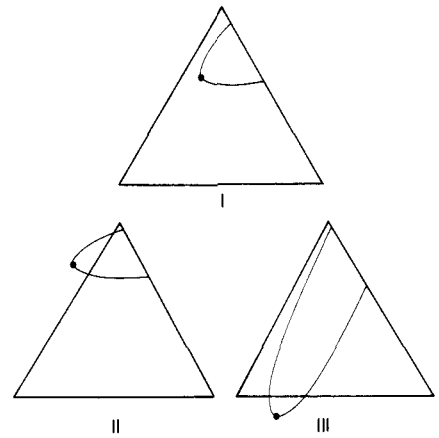

Figure 3. Phase diagram patterns I–III for quaternary systems with a single three-phase region: (●) stable triple critical point that may (I) or may not (II, III) be physically real. The curve indicates the HDPP line. Composition triangle orientation: component 1, top; 2, left; 3, right.

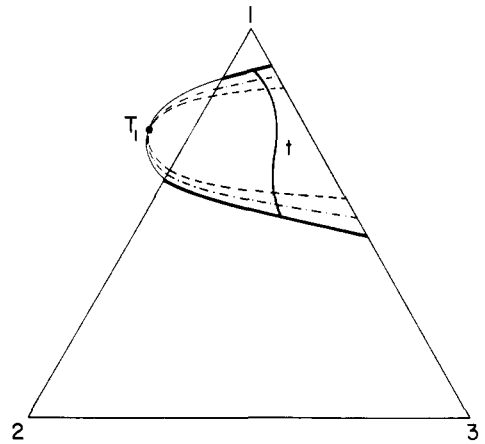

Figure 4. Sketch of some important lines in a phase diagram of a quaternary system type II: (T_1) stable but physically not real triple critical point; (—) three-phase boundary line; (- - -) critical end line; (- · -) HDPP line; (t) trinodal.

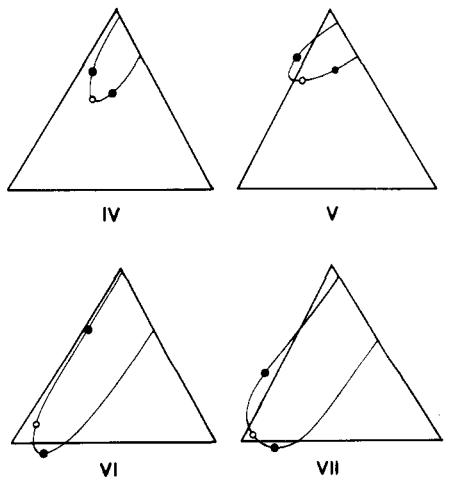

Figure 5. Phase diagram patterns IV–VII for quaternary systems with more than one three-phase region and possibly also a four-phase region: (●) (meta)stable triple critical points; (○) unstable triple critical point. The rest of the notation identical with that of Figure 3.

(for a finite r_1) in our previous report.[7] Cases II and III differ from I only in that two, rather than just one, of their constituent ternary systems show three-phase separations, and the three-phase region with the triple critical point T protrudes through one of the composition triangle axes, rendering T and its neighborhood physically not real. The topology of all important lines, however, stays unchanged, and they appear as single curves of simple shapes (see Figure 4). There is just one three-phase region enclosed by the three-phase boundary line. Continuing inward, we find the three-phase critical line or the critical end line[15] (the locus of compositions equilibrated with the three-phase boundary line), and the HDPP line, one curve entirely encasing the other, with the only common point of contact being the triple critical point. For each particular temperature, there is just one trinodal (locus of three-phase equilibrium compositions), anchored by its ends to the three-phase boundary line and serving as a "rail" guiding the tie triangles (triangular tie lines) whose apices slide along it as the solvent content of the system changes.

A qualitatively different situation, however, arises when the quadruple line in Figure 2 is crossed and two new triple critical points appear on the HDPP line. Since this curve cannot self-intersect, nor can it exist as an isolated loop,[7] it has to retain its simple character, and the only distinguishing feature among various types at this point can be the location of triple critical points. Consideration of the two points mentioned earlier leads to the classification into types IV–VII (Figure 5) characterized by more than one distinct three-phase regions, not necessarily all stable, and possibly overlapping and thus creating a four-phase region. If the respective constituent ternary systems split into three phases, one or both stable triple critical points may lie outside the composition triangle beyond the axes 1–2 and/or 2–3, never together beyond the same axis; but the unstable triple critical point stays inside. Mapping of the corresponding systems into α–β plane of Figure 2 is self-evident. Again, there are no basic differences between phase diagrams of various types of this class (IV–VII) except for the fact that (i) different portions of them may lie outside the composition triangle and (ii) whenever the HDPP line penetrates an axis, the quaternary pattern there has to smoothly connect into ternary behavior "within" this binary axis. Hence, it will be sufficient to examine only one type of diagram, say the type IV.

3.2. Finite Molecular Weights. The advantage of the high-molecular-weight limit, $r_1 \rightarrow \infty$, discussed in the preceding section was the simplicity and clarity of the resulting relations many of which could be expressed analytically. Cases with finite r_1 require more numerical work; nevertheless, they can be also easily analyzed.

The quadruple critical line is best computed again as a parametric curve from eq 12 and 13. Figure 6 shows results for $r_1 = 1, 3, 10$ and $r_1 \rightarrow \infty$. A decrease in r_1 leaves the character of the quadruple line practically unchanged, with the horizontal branch merely shifting upward and its asymptote always positioned at the ratio typical for the respective triple-critical ternary system; e.g., for $r_1 = 1$ the asymptote is at $\alpha \approx 15.645$. Surprising is the relative constancy of the vertical asymptotic branch and of the β-coordinate of the quintuple critical point (shifting merely from ≈ 3.10 for $r_1 \rightarrow \infty$ to ≈ 3.17 for $r_1 = 1$). Also the minimal value of r_z^* at the quadruple line (i.e., its parameter for $\beta \rightarrow \infty$) changes very little, from ≈ 1.816 to ≈ 2.057. Thus, it seems that after overcoming the first hurdle that is more difficult (namely, achieving three-phase separation in a ternary mixture), systems with low r_1 are just as eager to develop higher critical points and multiphase regions

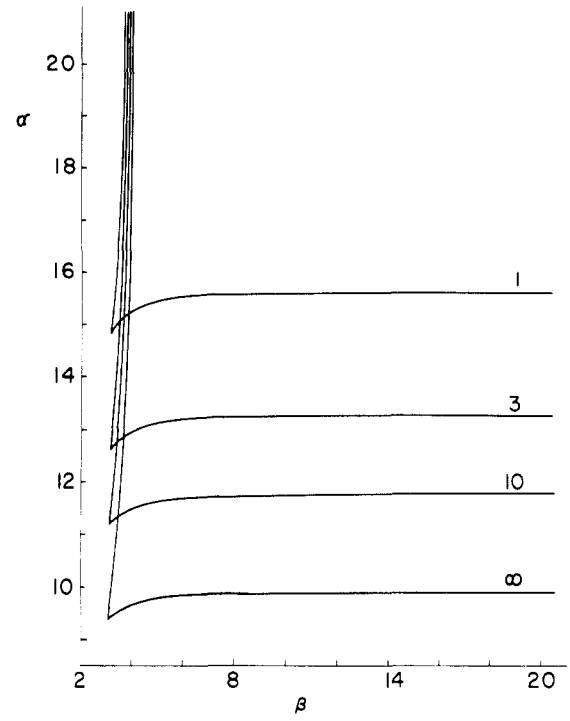

Figure 6. Dependence of the quadruple critical line on the size of the lowest component (r_1 indicated at each line). Coordinates α and β specify chain-length ratios r_2/r_1 and r_3/r_2, respectively.

by addition of higher homologues, as are systems with high r_1.

It is evident that also the rest of the discussion in the preceding section stays valid in principle for finite r_1, with only numerical values modified and dependent on r_1. The next section contains a detailed analysis of phase behavior for one such finite r_1 system.

4. Calculation of Multiphase Diagrams

In our experience, the best route to calculate three- and four-phase equilibria in polymer solutions is via their cloud point curves (CPCs). First, this type of phase diagram stays valid for any number of polymer components; second, its computation can be relatively easily automated. For a given molecular weight distribution of the polymer (i.e., a set of r_i's, and the mixture composition $\mathbf{w}$), its CPC is scanned for the presence of cusps. The scanning is done by successively incrementing the value of the separation factor σ and finding from the CPC equation in a single iteration cycle the corresponding volume fraction of the polymer ϕ (and the rest of variables).[4,6] Since σ changes monotonously along the CPC (even if this curve contains cusps), and the solutions ϕ are unique, there is a guarantee that no significant feature of the CPC escapes attention. Usually a cusp can be identified by reversal in the sequence of computed ϕ_j's (or χ_j's); e.g., with a positive increment $\Delta\sigma$, the calculated ϕ_j's normally keep decreasing, but after passing the first (or, generally, an odd) cusp, the increment $\Delta\phi$ turns positive. After a cusp is detected, its position is refined, and the scanning continues until the second (or, generally, an even) cusp is located and its position refined. From now on, the array of subsequently computed values ϕ_j, χ_j has to be systematically compared with array(s) of the previously computed and stored (meta)stable portions of the CPC, in order to locate and refine their intersection, a (meta)stable three-phase point. In ternary systems, the scanning can be interrupted after finding the first three-phase point, since a CPC cannot have more than one. In quaternary systems, however, the computer has to continue searching since there may be up to three different

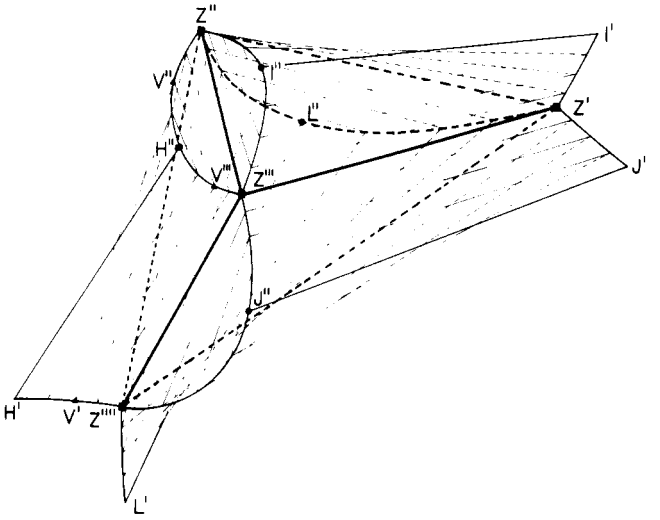

Figure 7. Isothermal phase diagram for a four-phase quaternary system in the full composition space: indicated is the four-phase tetrahedron (Z′Z″Z‴Z⁗) and four sets of three-phase equilibria (such as, e.g., V′V″V‴); (●) critical end points; arched curves and twin end lines at Z′ and Z⁗ represent a composite trinodal. For better clarity, binodals and tie lines associated with them are not displayed.

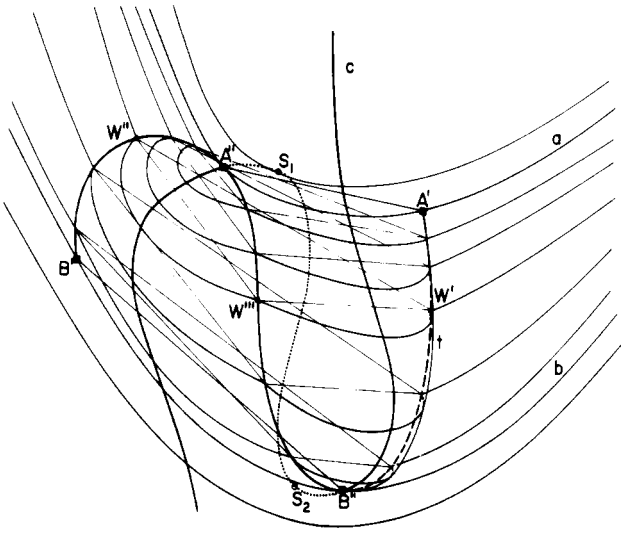

Figure 8. Part of the isothermal phase diagram for a three-phase quaternary system in the full composition space: (A″, B″) critical end points; (S_1, S_2) heterogeneous double critical points; (t) trinodal; (c) critical line; (a, b) binodals; (W′W″W‴) a three-phase equilibrium.

(meta)stable three-phase points. Evidently, at a four-phase equilibrium all of these three points merge into one.

Repetition of the above procedure for various polymer compositions **w** generates sets of data on parameters of coexisting phases at various temperatures, which can be manipulated according to one's objectives. For instance, for tracing a trinodal and its set of tie triangles, one aims for such compositions **w** that would yield a three-phase equilibrium at a particular temperature. The three-phase boundary line, on the other hand, is identified as the locus of compositions where the CPC just starts "breaking". Along this line, at the solvent content specified by the incipient break in CPC, the three-phase region is still infinitesimal, but a small composition perturbation $\delta\mathbf{w}$ "inward" results in a well-developed three-phase equilibrium. It is practically impossible to detect the incipient break directly from the sequence of χ_j,ϕ_j pairs; rather some well-defined criteria are used for this purpose. Information on the critical end points conjugated with the points of three-phase boundary line is obtained as a byproduct.[7]

One question might arise in the context of the above-described method: Is the set of phase equilibrium compositions derived in this way complete? Note that p-phase compositions are calculated exclusively as p-phase points of the CPC where $p - 1$ of its (meta)stable portions have a common point of intersection, and the phase volume ratios between the bulk and incipient phases go to infinity. In other words, this procedure assumes that each p-phase equilibrium can be accessed directly from the one-phase homogeneous state of the system, without first having to pass through two-phase, three-phase, etc., regions. This is of course very different from a typical path observed upon change in temperature where the system *does* pass through the above sequence of states with various numbers of phases. Fortunately, the concern turns out to be unwarranted. In the complete composition space the multiphase equilibria are projected as polygons of various dimensionality, aligned and stacked on top of each other. For instance, for a quaternary four-phase system at a given temperature, the equilibrium phases are represented by the apices of the four-phase tetrahedron (Z′, Z″, Z‴, and Z⁗ of Figure 7), and each mixture with its representative point inside the tetrahedron splits into these four phases in accord with the generalized lever rule. Stacked on each face of the tetrahedron is an infinite set of triangles (such as, e.g., V′V″V‴) corresponding to the continuous spectrum of three-phase equilibria that can exist at the given temperature. Each of the triangle sets in turn eventually degenerates at its critical end point (e.g., H″ of Figure 7) into a two-phase tie line (H′H″). Moreover, sets of two-phase tie lines mushroom along each edge of each triangle (e.g., Z′Z‴, V′V″, J′J″), in the manner similar to Figure 8, thus surrounding the displayed tetrahedron even more thoroughly. Yet, free access to all of the apices is preserved—since there is no way that a zero-dimensional apex could be aligned and "covered" with a one-dimensional line or two-dimensional triangle. Thus, while a typical path through the four-phase tetrahedron (whether induced by change in composition or temperature) indeed takes the system also through two-phase and three-phase regions, there always exist special trajectories that go directly from the one-phase state to a three-phase or four-phase region.

Figures 7 and 8 deserve a brief digression. The latter one is a more complete version than previously offered[13] of the isothermal phase diagram drawn in the full composition space for a three-phase quaternary system. The three-phase region, at this particular temperature entirely isolated within the tetrahedron of compositions, grows on the binodal surface[16] as a pair of oppositely oriented "droplets". The left new binodal system is rooted at the heterogeneous double critical point S_1 located under the binodal surface. Proceeding downward, the new binodals keep growing until they touch from inside the old binodal surface (at the critical end point A″) and eventually protrude through it. At the same time, starting with the binodal a, these curves develop a cusp system on the right-hand side (point A′) that is externally perceived as a break in an otherwise smooth curve. Both above features form the basis for three-phase equilibria, just as they did in the case of temperature variation of ternary binodals. In fact, the analogy is even deeper: In both cases the binodals pass through a symmetric pattern (cf. Figure 3d of ref 6) and finally switch the sides, to create a new binodal on the right and a cusp system on the left, which eventually disappear from the stable surface at the binodal level b (with the critical end point B″). The metastable and unstable residues of the right binodal system then

Table II
Approximate Values of Composition and Temperature for Some Significant Points of the Diagram in Figure 9

point	w_2	w_3	χ
T_1	3.94×10^{-2}	1.09×10^{-3}	0.859 278
T_2	1.58×10^{-2}	4.21×10^{-5}	0.862 413
T_3	7.79×10^{-3}	3.60×10^{-8}	0.862 148
B′	6.44×10^{-2}	1.3×10^{-2}	0.862 212
B‴	2.26×10^{-2}	1.5×10^{-4}	0.862 212
B″	5.8×10^{-3}	5×10^{-7}	0.862 212
A′	6.54×10^{-2}	1.42×10^{-2}	0.862 264
A″	1.38×10^{-2}	2.0×10^{-5}	0.862 264
A‴	3.3×10^{-3}	5.2×10^{-8}	0.862 264

shrink to a point at the heterogeneous double critical point S_2. Winding its way through the three-phase disturbance is the line of critical points c that is only partly stable (i.e., located on the binodal surface); parts A″S_1 and B″S_2 are metastable, and S_1S_2 is unstable. The S-shaped line t, the locus of three-phase equilibrium compositions, is the trinodal of Figure 4.

Note that the three-phase region in a quaternary system does not have to be always complete as depicted in Figure 8. For instance, at lower temperatures one of its triangles becomes coplanar with the 0–1–3 face, leaving part of the region outside the tetrahedron.

Figure 7 for a four-phase quaternary system is incomplete, lacking for reasons of better clarity the binodal surface background into which the displayed body would be embedded. Indicated, however, is the trinodal as a composite curve, partly single, partly split in two, embracing the four-phase tetrahedron, with four critical end points L″, I″, H″, and J″ on it. The critical line would run here on the not displayed binodal surface to the critical end point J″, then plunge beneath it and emerge at H″, continue as a stable curve toward I″, submerge once more, and finally reappear at L″. These unusual patterns will become more obvious in section 5.1.

Numerical computations are sometimes rather delicate; particularly the choice of σ increment for CPC scanning may be critical. It is evident that small cusp systems may be easily missed if $\Delta\sigma$ is too large. On the other hand, with $\Delta\sigma$ too small the round-off errors in results might give a false signal of a CPC reversal where none actually exists. However, with proper choice of this parameter (in our case mostly $\Delta\sigma \approx (3\text{–}5) \times 10^{-4}$), and using double-precision arithmetics on the 16-bit HP 1000 computer, we were able to identify reliably even cusp systems extending over an interval of only 2×10^{-6} in ϕ and less than 1×10^{-6} in χ. The consistency of the results is easily checked by choosing incipient phases resulting from the first calculation as bulk phases for the subsequent calculations; the equilibrium parameters obtained should be of course the same.

5. Quaternary Four-Phase Systems

The following section gives a detailed account of the simplest four-phase case, namely the type IV of Figure 5 where all important features of the phase diagram are contained within the triangle of polymer compositions. Phase behavior of other quaternary systems is briefly discussed in section 5.2.

5.1. Quaternary System 10/117.6/450. As an example of the type IV quaternary system, we analyzed the case with polymer chain lengths $r_1 = 10$, $r_2 = 117.6$, $r_3 = 450$ (i.e., $\alpha = 11.76$, $\beta \approx 3.827$). Presenting the actual phase diagram on the scale acceptable for publication would accomplish little since the interesting features are spread over several orders of magnitude in w_3. Hence, we shall use for the discussion a schematic drawing displayed in Figure 9 that is topologically equivalent to the actual

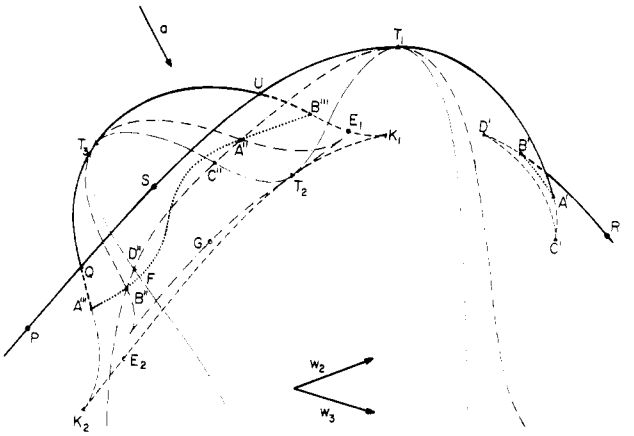

Figure 9. Scheme of the phase diagram for the quaternary system 10/117.6/450, drawn in the polymer composition space w; general direction of the composition axes w_2 and w_3 is shown by arrows: (bold line) stable three-phase boundary line, its full and dashed portions indicating visibility of the two trinodal surfaces when viewed from the top, against the temperature axis; (- - -) metastable and unstable portions of the three-phase boundary line; (— — —) HDPP line; (· · ·) critical end lines; (···) four-phase lines. Arrow a indicates the view direction for the temperature plot of Figure 11a.

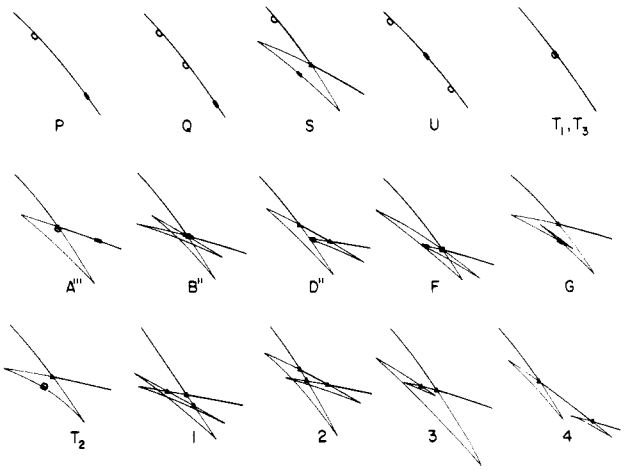

Figure 10. Schematic drawing of characteristic portions of some cloud point curves. Letters and numbers specify the position of the representative points of the polymer mixtures in the diagrams of Figures 9 and 11b, respectively: (—) critical point, with the bar indicating the direction of the CPC branch to which it is attached; (○) incipient break on the displayed portion of the CPC; (▲) a (meta)stable three-phase point; (■) a four-phase point. Note that, technically, incipient breaks are also three-phase points, although they are not so designated here to avoid confusion.

pattern but has distorted coordinates. Actual values of some variables at some special points are listed in Table II.

As indicated above, various features of the phase diagram have been traced from the CPCs for the respective polymer mixtures, and the assignments between the two should be obvious. For instance, point Q, in the projection of Figure 9 an apparent intersection of two three-phase boundary lines (that in fact are separated in temperature space), is characterized by two incipient breaks in Figure 10. The mixture D″ has to have its critical point located at a cusp (D″ is on the HDPP line), simultaneously overlapping with another CPC branch (D″ is also on a critical end line), and it has to possess two stable three-phase points. Similar arguments can be extended to all other features, and they have to result in CPC patterns that exhibit continuous changes as one moves in the phase diagram from one point to another.

Two new features appear in Figure 9, compared to the simplest case with a single triple critical point (such as discussed in ref 7, or displayed in Figure 4): (i) a "new" two-cusp loop of three-phase boundary line together with its conjugated inner loop of critical end points, developed around the pair of new triple critical points T_2 and T_3 on the left, and (ii) the concomitant two-cusp system generated on the distant branch of the "old" three-phase boundary line on the right. Note that the loop has developed around the original deformed HDPP line; in fact, this is the only possible way. No new separate HDPP line could have been generated as this line (i) cannot exist in the form of a closed loop and (ii) cannot self-intersect.[7]

Formally, the diagram resembles the isothermal pattern of binodals for a three-phase ternary system, with the following analogies: three-phase boundary lines ↔ binodals; the HDPP line ↔ spinodal; triple critical points ↔ single critical points. In fact, the similarity extends to some more subtle points; e.g., in Appendix 2 it is shown that the cusps C′ and D′ of the three-phase boundary line have to be conjugated with points C″ and D″ of the HDPP line, just as cusps of binodals for ternary systems are equilibrated with points of the spinodal. On the other hand, there are some significant differences: The triangular w-space is only an incomplete representation of the quaternary system. Hence, the three-phase boundary line is not conjugated "with itself" as binodals are, but with a separate curve—the line of critical end points.[7] Moreover, since a three-phase quaternary liquid system has two degrees of freedom, the temperature alone does not specify the equilibrium phases; rather, for each temperature, one has to define an infinite array of three-phase equilibrium compositions (i.e., the trinodal) along which the tie triangles slide in predetermined fashion. Another difference is in all of the displayed features of Figure 9 being nonisothermal, whereas the binodal patterns in ternary systems are drawn for constant temperature. Yet, the change in the pattern of Figure 9 due to varying chain-length ratio(s) again closely resembles the effect of temperature on binodal patterns in ternary systems (see below).

The best way to view the diagram of Figure 9 is to expand it into three dimensions, with the added parameter χ (i.e., temperature) plotted perpendicularly to the polymer composition triangle base. In such a space, the locus of three-phase equilibrium compositions is a surface—call it the trinodal surface—bounded by the three-phase boundary line. Contained in this surface are also all features of Figure 9—except for the HDPP line that generally runs without it, contacting it at some specific points (e.g., at triple and higher critical points).

The distinction between a system with a single three-phase region and the present four-phase system in the temperature space is striking. Whereas formerly there was just a single trinodal surface, smooth and well-behaving,[7] in the latter case the two-cusp loop represents the boundary of a newly generated surface cutting through the old one, with the line of intersection A‴B‴ forming one branch of the four-phase line (i.e., of the locus of four-phase equilibria). The temperature profile of this two-cusp loop is quite complex, and it is displayed in Figure 11a. The absolute maximum and minimum correspond to the above-mentioned triple critical points, the stable T_3 and unstable T_2, respectively. In addition, the cusp K_1 (positioned closer to the triple critical point T_1) is pointed upward while K_2 is directed downward, which leads to the existence of two local extrema E_1 and E_2. The line of intersection of the two surfaces is S-shaped, with its end points A‴ and B‴ conjugated with its extrema A″ and B″,

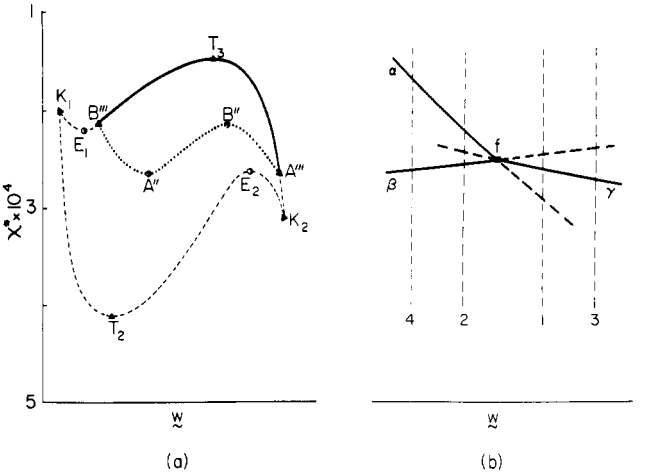

Figure 11. Temperature profiles of some portions of the trinodal surface for the 10/117.6/450 quaternary system. Only the temperature coordinate χ^* for part a is drawn to scale, where $\chi^* = \chi - 0.862$. a: new T_3 trinodal surface; (—) stable and (- - -) not stable portions of the three-phase boundary line; (···) four-phase line. Point notation is identical with that of Figure 9. b: Cross section of the trinodal surfaces in the neighborhood of the four-phase line f; outer stable surfaces, α and β; inner stable surface, γ; (- - -) metastable continuation of surfaces. CPCs of mixtures specified by the numbers 1–4 are displayed in Figure 10.

respectively. Relative to the old trinodal surface, the stable outer portion A‴T_3B‴ of the loop is positioned under the "rim" T_1P, while the metastable and unstable portions A‴$K_2E_2T_2K_1E_1$B‴ protrude actually above the original surface. Note that the presence of the new surface also deforms the old one which is no longer smooth; along the four-phase line its slope exhibits a discontinuity that vanishes only at the end points A‴ and B‴.

Another complex feature arises on the right-hand side of Figure 9, where the double-cusp system represents a projection of a "split-in-two" trinodal surface. The branch A′T_1 of the three-phase boundary line ascending toward the triple critical point T_1 here overlays the other branch B′R, and the two corresponding surfaces intersect in the monotonously increasing ling A′B′ that constitutes another locus of four-phase equilibria. The inner original stable part of the trinodal surface meets the above two outer split surfaces generally at angles other than 180°, and only at the end points A′ and B′ is it smoothly connected to one of them—specifically, to the upper one at B′, and to the lower one at A′.

A careful reader will notice that the above account of trinodal surfaces in the neighborhood of the four-phase line cannot be complete; the continuity condition for CPC patterns clearly requires that the three stable surfaces mentioned above (e.g., the new surface bounded by A‴T_3B‴, and the outer and inner portions of the old trinodal surface) continue beyond their common line of intersection as metastable states. The situation is illustrated in Figure 11b, with some typical CPC patterns again in Figure 10. Cloud point curves of mixtures around the four-phase line consist of three (meta)stable portions (plus two unstable parts), and crossing the line, say outward, shifts the middle metastable part higher relative to its neighbors. Thus, the CPC of the polymer mixture 1 located just inside the four-phase line contains one stable and two metastable three-phase points, corresponding to one stable and two metastable trinodal surfaces. By moving closer to the four-phase line, these three points approach and eventually merge together in a common point of intersection of all three (meta)stable CPC portions

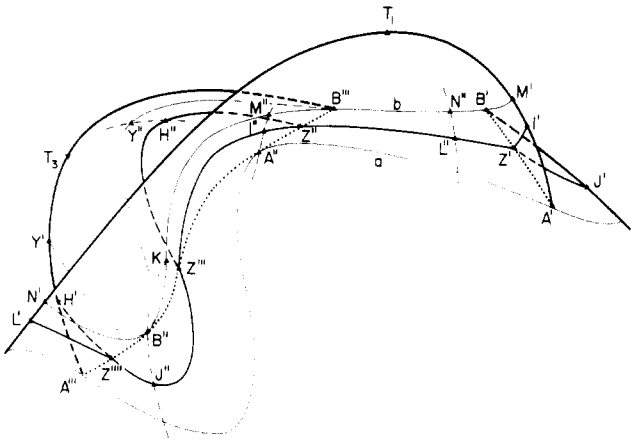

Figure 12. Phase diagram of Figure 9, with some of the lines omitted, and slightly modified to display with better clarity three trinodals marking the following: (b) the onset of four-phase region; (bold line) well-developed four-phase equilibrium; (a) the end of four-phase region. Notation for the rest of lines (including portions of critical end line) is identical with that of Figure 9; the points are consistent with Figures 7 and 9.

(i.e., in a four-phase point). Here the CPC acquires the pattern displayed in B″ of Figure 10, although in general the critical point may be located anywhere on it. Finally, a further shift outward (mixture 2) creates two stable and one metastable three-phase points, again located within the corresponding trinodal surfaces. It is, however, apparent that the situation as described for immediate neighborhood of the four-phase line cannot continue indefinitely. On the outer side, the two stable three-phase points of the CPC move apart from each other and the metastable one soon ceases to exist, as follows from the pattern sequence 2,4 of Figure 10. Similar development occurs inside the four-phase line where both metastable three-phase points eventually vanish, certainly before crossing the unstable lines K_1K_2 or C′D′ (Figure 9), as displayed for one of such points in the sequence 1,3. An interesting conclusion of the above argument is that there is a discontinuity in the surface between the four-phase line (say A‴B‴) and the unstable portion of its corresponding three-phase boundary line (K_2K_1)—although the latter line itself is continuously connected through the cusps to the former one. Rather the four curves forming a closed loop (A‴B‴K_1K_2) are merely lined with residues of surfaces generated by various types of three-phase points [(meta)stable and unstable], with a gap in the middle of the loop. Fortunately all these complex features can be ignored if only stable equilibrium states are of interest.

Let us now turn our attention to changes that occur in the system with decreasing temperature. At high temperatures, $T_{T_3} < T < T_{T_1}$, there is just one three-phase region present, rooted in the triple critical point T_1. Trinodals span the main arc of the three-phase boundary line around T_1 as usual,[7] without interference with the cusp system and the loop located below. At the temperature of the critical point T_3 a new three-phase region starts developing around it, seemingly unrelated to the first one, and proceeds inward with further cooling of the system.

The first time the trinodals of these two regions interact is at the temperature corresponding to points B, the upper extreme points of both four-phase lines. Here the trinodal of the first set (thin line b of Figure 12) starts at M′, passes through B′ and B‴, then turns down, contacts "from outside" the four-phase line at B″, and finally ends at the three-phase boundary line at N′. Note that the points B″ and B‴ are the first of their kind; at a temperature infinitesimally higher there are no stable analogues to these points, and the trinodal (shifted up and left) would exhibit only normal critical end points, like M″ and N″, conjugated with boundary points M′ and N′. Actually the new point B″ is also a critical end point, associated however with the lower branch B′J′ of the right descending three-phase boundary line. The other trinodal belonging to the T_3 set starts at B‴, swings up and down the T_3 surface, passing through Y″, also contacts the four-phase line at the critical end point B″, and finally ends at Y′. It is apparent that it lies in a surface different from the first trinodal, and the only common points of the two are the points B″ and B‴ of the intersection line. One could also view these two curves as one composite trinodal that runs singly in parts of the original surface, but splits in two wherever it encounters another stable surface growing out of the four-phase line. Strictly speaking, at this temperature there still can coexist no more than three phases (e.g., B′, B″, and B‴), but note that the critical end phase B″ is on the verge of being split in two.

A well-developed four-phase equilibrium is characterized by a composite trinodal that splits in two in its middle portion and at the ends, but runs singly between (bold line in Figure 12). Interesting is the asymmetry of the entire event: The right four-phase line resulting from a split in the old T_1 surface is monotonous in temperature, thus displaying always only one of the four equilibrium phases (Z′). On the other hand, the four-phase line generated by the new trinodal surface on the left is S-shaped (cf. Figure 11a) and contains three conjugated phases (Z″, Z‴ and Z⁗), with each restricted to the respective parts of the curve (B‴A″, A″B″, B″A‴). At first sight, the complex topology of this trinodal does not seem to offer much physical insight. From its full representation in the isothermal complete composition space of Figure 7, however, it becomes clear that this is probably the only way that a continuous curve can encompass the four-phase equilibrium as well as an entire spectrum of three-phase equilibria existing at a given temperature. Four points of intersection of the trinodal with four-phase lines of Figure 12, Z′, Z″, Z‴, and Z⁗, are in fact projections of the apices of the four-phase tetrahedron. Each arc of the trinodal (twin arcs between Z″ and Z‴ in the middle, and two single ones Z′Z″ and Z‴Z⁗) is associated with one of the four free ends, thus forming loci for apices of three-phase triangles surrounding the tetrahedron. Assignments between various arcs and free ends can be done by utilizing critical end points. For instance, the boundary point L′ is conjugated with the critical end point L″; hence, the free end Z⁗L′ belongs to the arc Z′Z″. The free end H′ can be associated only with the arc Z″H″Z‴ since both of them lie within the new surface around T_3. Finally, the coexistence of points I′ and I″ indicates that the upper free end of the trinodal on the right is tied to the remaining twin arc Z″I″Z‴, while a similar argument points to the conjugation between the lower free end Z′J′ and the single arc Z‴Z⁗. The reader might notice the existence of an apparent third point of intersection between the trinodal and the left branch of the critical end line such as, e.g., K; it turns out that this point is physically meaningless since it corresponds to an unstable state.

Changes observed upon further cooling should be now evident. The composite trinodal of Figure 12 moves further right and down, and its split portions (equivalents of Z′I′, Z″I″Z‴, Z″H″Z‴, and Z⁗H′) are getting smaller. At T_A the T_1-trinodal reaches the other extreme point A‴ of the left four-phase line, its middle loop just touches this line "from inside" at the critical end point A″, and on the right-hand side it passes through the point A′ (curve a in

Figure 12). It thus becomes once again a simple-shape curve with no discontinuities in slope. The trinodal on the new T_3 surface has receded at this temperature entirely into its metastable and unstable parts, and eventually it would disappear in the unstable triple critical point T_2. The existence of a four-phase equilibrium is thus restricted to a narrow temperature interval between $\chi_B \approx 0.862212$ and $\chi_A \approx 0.862264$.

The above account sheds light on the mechanism of four-phase separation as viewed in the complete composition space of Figures 7 and 8. The notation in the series of isothermal snapshots in Figure 13 is necessarily somewhat inconsistent with diagrams of Figures 9 and 12, since some points distinguished in the latter nonisothermal projection for the purpose of discussion (e.g., M″, I″, and A″) are in fact the same point in different development stages when viewed in the sequence of diagrams of Figure 13.

Figure 13a depicts two seemingly independent three-phase regions present at higher temperatures. Critical end point notation corresponds to that of Figure 7, with the exception of the point β that does not survive as such the formation of the tetrahedron. With diminishing temperature the regions approach each other, until at T_B they form a linear contact (Figure 13b). Note that the contact is made in a very specific way, between the critical end tie line β of the left T_3 set, and one of the sides of triangle B of the right T_1 set (cf. also Figures 9 and 12). Further decrease in temperature drives the T_3 three-phase region into the T_1 region; this is accompanied by splitting of the critical end phase β'' in two common equilibrium phases, Z‴ and Z⁗, and simultaneous opening of the triangle B into a tetrahedral form as shown in Figure 13c. Although the trinodal arc around β'' and the associated free end β' have been absorbed at this stage by the tetrahedron, one cannot say the same about the critical end point β'' itself: critical end points are by definition on the boundary between stable and metastable states and thus cannot become purely metastable or unstable. The point β'' rather switches its allegiance to the newly formed arc, thus earning a new label J″. This can be clearly seen in the CPC projection of Figure 10, pattern B″, where the critical point positioned on the high-concentration branch indeed can choose between equilibrium involving another point on the middle branch or one on the low-concentration branch. Thus, the total number of critical end points—four—stays unchanged in the process of merging the two three-phase regions into a four-phase region.

Final outcome of reducing the temperature is obvious: the left three-phase region (originally belonging to the T_3 set) keeps moving into the tetrahedron, with the Z″Z‴ edge, as well as its twin arcs, and free ends H′ and I′, becoming eventually shorter until they disappear at temperature T_A. At this point, the four-phase equilibrium has degenerated into a three-phase region. The overlap of points Z″, Z‴, H″, and I″ becomes A″ of Figures 9 and 12, which is the last critical end point in the sequence; at even lower temperature only the critical end points J″ and L″ remain, as is appropriate for a single three-phase region. Its behavior is then normal all the way to the 1–3 axis of the polymer composition triangle (i.e., 0–1–3 face of the composition tetrahedron).

5.2. Other Four-Phase Systems. From the above discussion it follows that the existence of a four-phase region in a given system is tied to the occurrence of an additional stable three-phase region that, although at higher temperatures seemingly independent (i.e., located in a different composition range), is in fact rooted in the primary three-phase region at lower temperatures. A four-phase equilibrium thus appears for the first time in a system where the new T_3 trinodal surface, at first not stable, just contacts the established T_1 surface. Further signs of such a system are the following: (i) both four-phase lines degenerate into points; (ii) two cusps C′ and D′ of the right boundary line merge into a double-cusp

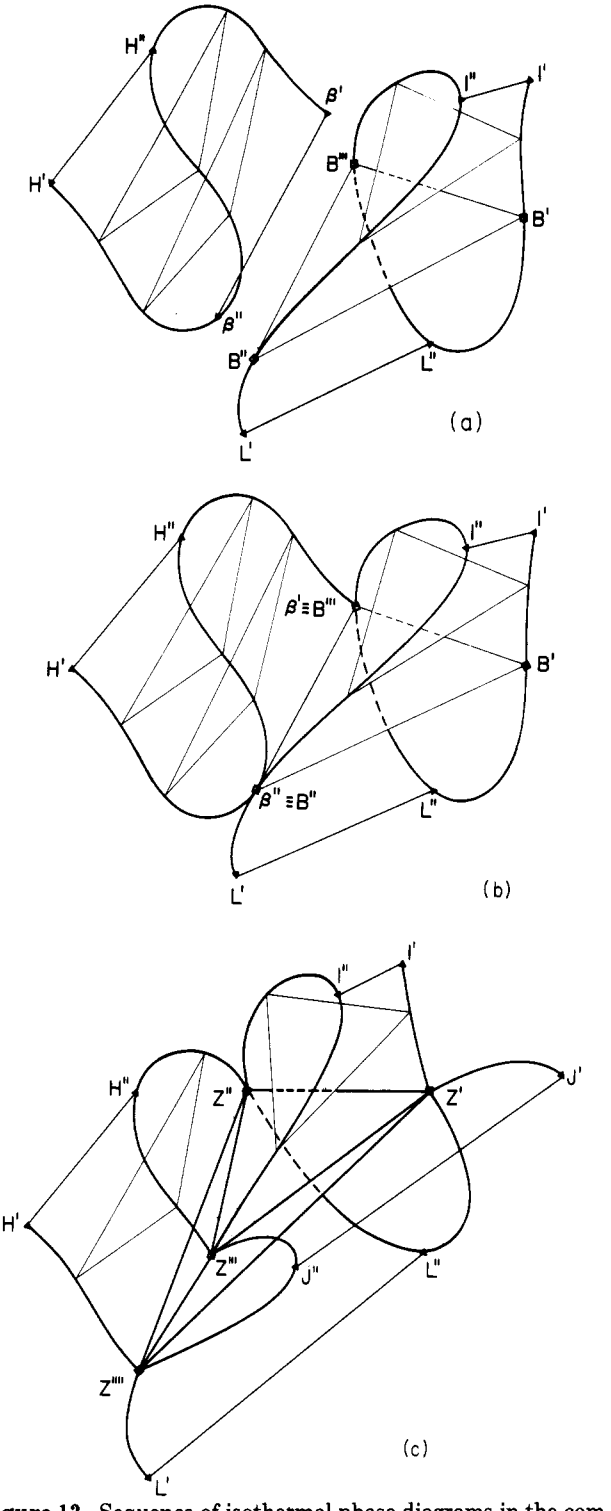

Figure 13. Sequence of isothermal phase diagrams in the complete composition space describing the effect of diminishing temperature, and the formation of a four-phase region. Set of triangles associated with T_1 is on the right, while that belonging to T_3 is on the left: (bold line) trinodal; (medium line) critical end tie line; (thin line) triangular tie line. The four-phase tetrahedron in part c is also drawn in bold line. Point notation is explained in text. a: $T_B < T < T_{T_3}$. b: $T = T_B$. c: $T_A < T < T_B$.

point. An important corollary to the latter statement is that the point of first contact between old and new surfaces has to be a stable triple critical point. Since a simple cusp is conjugated with a double critical point (see Appendix 2), then a double cusp has to coexist with a double point of the HDPP line, i.e., with its extremum, a triple critical point. It is probably impossible to derive explicit criteria for this case, say in terms of chain length r_1 and ratios α and β (as we did for the quadruple critical line), since one has to search for a triple critical point that can coexist with a distant phase—a problem that could be tackled only numerically by solving unexpanded equations. It is evident, however, that such a condition is not the same as that for quadruple critical points which by definition lie deep in the metastable–unstable region.

The sequence of events when crossing the quadruple line has to be as follows: In the regions I–III of Figure 2, the system has just a single three-phase region and one triple critical point, and its behavior is simple.[7] At the quadruple line, the pair of newly created, still overlapping triple critical points is deep below the stable portion of the respective CPC; i.e., neither one of them can be stable. A small increase in one of the chain-length ratios separates triple critical points T_2 and T_3 from each other, and the new trinodal surface around them assumes a finite size; yet it did not grow far enough to touch or penetrate the old surface, and none of its features is thermodynamically stable. In general, it takes a further increase in chain-length ratios to achieve conditions similar to those of Figure 9, with one four-phase and two separate three-phase regions. Both asymptotic branches of the quadruple line of Figure 2 are thus lined with a "transition" area of systems with two three-phase regions only one of which is stable, and only the middle portion of the cusp area can be designated as the four-phase region proper.[8] All three areas converge at the cusp of the quadruple line, i.e., at the quintuple critical point. This point represents the "lowest" possible system that could ever show a four-phase equilibrium (although its range would only be infinitesimal). It also represents the only quaternary system where, at the quintuple critical point, four phases become critically identical.

As follows from patterns of triple critical points in Figure 5, the phase diagram of a system IV is not necessarily always of the type portrayed in Figure 9; the relative positions of triple critical points T_1 and T_3, as well as of the loop and the cusp system, can be switched. Also, since one can cross the region IV in Figure 2 from one to another branch of quadruple line in a continuous fashion, there has to exist a system with a symmetrical pattern, where the cusp K_1 of the loop of Figure 9 would merge with the upper cusp D′ of the right cusp system—something analogous to the symmetrical binodal pattern in ternary systems (cf. Figure 3d of ref 6). Another modification of the phase diagram is shown by systems which have one or both stable triple critical points beyond the triangle axes, i.e., physically not real (types V–VII). None of these changes, however, do affect fundamental relations between various lines of the diagrams in Figures 9 and 12 which can thus serve as universal examples for quaternary systems composed of a solvent and three homopolymer fractions.

6. Conclusions

General criteria developed earlier for triple, quadruple, and quintuple critical points have been applied to quaternary systems solvent (0) + three polymer homologues of chain lengths $r_1 < r_2 < r_3$. For this case, they can be recast in a much more compact and physically intelligible way, in terms of a single polymer-composition-dependent variable, and some quantities characterizing the system.

In the limit of very high polymer molecular weights, these relations are further simplified and can be examined to a large extent analytically. The results are best presented in the form of a critical point diagram where, in coordinates $\alpha \equiv r_2/r_1$ vs. $\beta \equiv r_3/r_2$, systems with triple, quadruple, and quintuple critical points are mapped as surfaces, lines, and a point, respectively. Thus, the occurrence of triple critical points is common, whereas the other two types of multiple critical points are very rare ("lucky accidents" in Griffiths words[11]). A quintuple critical point appears only in a system with $\alpha \approx 9.384$ and $\beta \approx 3.096$, while a quadruple critical point demands a specific value of α in the range $9.384 < \alpha \leq 9.899$ if $\beta > 3.096$, or a specific value of β in the range of $3.096 < \beta \leq 4.442$ if $\alpha > 9.384$. Somewhat surprising is the low value of β, compared to α, sufficient for the appearance of higher critical points. This suggests that the existence of multiphase equilibria in polycomponent systems should require a much lower overall chain-length ratio than one would expect at first sight.

Since multiple critical points are closely tied to multiphase equilibria, the above critical point diagram can also serve for classification of quaternary systems based on their phase behavior. Three types of phase diagrams are distinguished for three-phase systems, and four types can be identified for four-phase systems.

The above statements are generally valid even if the polymer molecular weights are finite, only specific numerical values are modified. For instance, for the other extreme, $r_1 = 1$, the quintuple critical point coordinates are $\alpha \approx 15.645$ and $\beta \approx 3.17$. While the relatively large change in α could have been anticipated from the ternary system theory, surprising is the very small effect ($\approx$2.3%) observed for β. It shows that, in a sense, the low-molecular-weight systems are just as eager to display higher critical points and multiphase equilibria as the high-molecular-weight systems are.

A four-phase diagram has been computed for the system $r_1/r_2/r_3 = 10/117.6/450$ (i.e., $\alpha = 11.76$, $\beta \approx 3.827$). The trinodal surface (i.e., the locus of three-phase equilibrium compositions plotted in coordinates temperature vs. the composition of polymer mixture) is no longer simple and smooth as it was for systems showing only a single three-phase region. Rather an additional new surface has grown around the pair of new triple critical points T_2 and T_3 and penetrates the original surface associated with the triple critical point T_1. Simultaneously, the original surface becomes split in two in some remote range of polymer compositions. In both cases, the lines of intersection of the two surfaces represent the four-phase lines, i.e., loci of four-phase equilibrium points. Interesting is the asymmetry of the diagram: while the line created by the new trinodal surface always contains three coexisting phases, the other line arising from the split surface carries only the remaining single phase. Formally, the genesis and development of this complex phase diagram strongly resemble the temperature variation of binodal patterns observed for ternary systems.

Analysis of results leads to the following mechanism of four-phase separation upon cooling the system (assuming the usual case of $d\chi/dT < 0$). At high temperatures, $T_{T_3} < T < T_{T_1}$, the system exhibits just a single three-phase region tied to the triple critical point T_1. At T_{T_3}, the temperature of the triple critical point T_3, another stable three-phase region starts growing around T_3, which is seemingly unrelated to the first observed region. With diminishing temperature, however, the two regions grow

closer to each other, until at T_B they make a linear contact in a specific way: a common side of a tie triangle of the T_1 set merges with one of the critical end tie lines of the T_3 set. Further temperature reduction causes penetration of the two three-phase regions, moving the T_3 set into the T_1 set that consequently "opens up", and the whole entity assumes the familiar tetrahedral shape typical of four-phase equilibria. Finally at T_A, the T_3 three-phase region has just been absorbed by the original T_1 set, with the last common line being again a critical end tie line of the T_3 set; the four-phase tetrahedron degenerates into a three-phase triangle, and hereafter the system possesses just a single regularly behaving three-phase region.

Although in other quaternary systems the phase diagram may be oppositely oriented, or parts of it may lie outside the physically significant triangle of compositions, the fundamental relations described above should stay generally valid.

In regard to the question raised in the Introduction, this and other[14] investigations suggest that theoretically there is indeed no limit to the number of phases one could observe in quasi-binary polydisperse systems with properly selected components, other than the trivial one—the number of components as stated by the Gibbs phase rule. With growing number of components (and phases), however, the temperature and composition ranges of the existence of such separations are bound to become smaller and smaller, and it is questionable whether one could in fact detect them experimentally.

Acknowledgment. Technical help with some calculations and with graphic work by Mike Rozniak is gratefully appreciated.

Appendix 1

We wish to derive the sign of change in the critical interaction parameter when advancing from a binary axis of the polymer composition triangle inward along the HDPP line. The change in χ_c due to a perturbation in polymer composition is[7]

$$d\chi_c = [(\Delta r_2^2\, dw_2 + \Delta r_3^2\, dw_3) \times (1 - r_w/r_z) - (\Delta r_2\, dw_2 + \Delta r_3\, dw_3)(3r_z - r_w)]/4r_z^{1/2}r_w^2 \quad (A1)$$

where Δr_k^2 stands for $r_k^2 - r_1^2$. Now, the r_w average in the brackets can be expressed in terms of r_z by using the binary equivalent of the ternary formula (6)

$$r_{z+i} = R - P/r_{z+i-1}$$
$$R = r_k + r_j, \quad P = r_k r_j \quad (A2)$$

while the newly introduced P can be substituted from eq A2 written for r_{z+1} (i.e., with $i = 1$), and from eq 2 valid at the HDPP line. For the high-molecular-weight limit, the result is

$$d\chi_c = [(\Delta r_2^2\, dw_2 + \Delta r_3^2\, dw_3) - R(\Delta r_2\, dw_2 + \Delta r_3\, dw_3)]r_z^{1/2}/2r_w^2(R - r_z) \quad (A3)$$

where the denominator term $R - r_z > 0$. The sign of $d\chi_c$ is thus equal to the sign of the bracket.

Application of eq A3 to the three binary axes then gives

$$d\chi_{c,13} < 0, \qquad d\chi_{c,12} > 0, \qquad d\chi_{c,23} > 0 \quad (A4)$$

The first relation has been derived in a different fashion also in ref 7.

Appendix 2

One of the conditions for a double cusp point of the CPC (i.e., for any point of the three-phase boundary line) is[5,6]

$$\phi/(1 - \phi v_0) = v_2^{1/2}/v_1^{3/2} \quad (A5)$$

where ν_k is the k-th moment of the chain-length distribution of the polymer contained in the conjugated incipient phase

$$\nu_k = \sum_{m=1}^{3} w_m r_m{}^k \exp(\sigma r_m) \quad (A6)$$

and σ is the separation factor.

At a cusp point of the three-phase boundary line, the composition variables $\mathbf{w}$ are fixed, and the only quantity of the right-hand side of eq A6 allowed to change when the line "turns around" is σ; hence

$$d\phi|_{cusp} = \left(\frac{\partial\phi}{\partial\sigma}\right)_{\mathbf{w}} d\sigma = \tfrac{1}{2}\phi^2 \frac{\nu_1^{3/2}}{\nu_2^{1/2}}(r_{z+1}^* - 3r_z^* - 2r_z^{*1/2})\, d\sigma \quad (A7)$$

where the asterisks specify quantities relating to the conjugated phase, and the expression in the parentheses is recognized as the condition for the double critical point, eq 2. But, the derivative $d\phi/d\sigma$ at a cusp point of the CPC has to be zero; hence, the point coexisting with a cusp of the three-phase boundary line has to be the intersection of the critical end line with the HDPP line.

Similar arguments applied to the relation for the composition of the conjugated phase

$$w_k^* = w_k \exp(\sigma r_k)/\nu_0 \quad (A8)$$

show that, in general, $d\mathbf{w}^*$ is nonzero even for the cusps of a three-phase boundary line where $d\mathbf{w} = 0$. This means that the critical end line stays well-behaving at the points that coexist with cusps of the three-phase boundary line. Again, this behavior is analogous to the spinodal staying smooth at points conjugated with cusps of the binodals in ternary systems, and the shadow curve staying smooth at the points conjugated with the cusps of the CPC for any polydisperse polymer.

References and Notes

(1) Tompa, H. *Trans. Faraday Soc.* **1949**, *45*, 1142.
(2) Koningsveld, R.; Staverman, A. J. *Kolloid Z. Z. Polym.* **1966**, *210*, 151; **1967**, *220*, 31.
(3) Koningsveld, R.; Kleintjens, L. A.; Shultz, A. R. *J. Polym. Sci., Part A-2* **1970**, *8*, 1261.
(4) Šolc, K. *Macromolecules* **1970**, *3*, 665.
(5) Šolc, K. *Macromolecules* **1977**, *10*, 1101.
(6) Šolc, K. *J. Polym. Sci., Polym. Phys. Ed.* **1982**, *20*, 1947.
(7) Šolc, K. *Macromolecules* **1983**, *16*, 236.
(8) Šolc, K.; Kleintjens, L. A.; Koningsveld, R. *Macromolecules* **1984**, *17*, 573.
(9) Flory, P. J. "Principles of Polymer Chemistry"; Cornell University Press: Ithaca, NY, 1953; Chapter XIII.
(10) Stockmayer, W. H. *J. Chem. Phys.* **1949**, *17*, 588.
(11) Griffiths, R. B. *J. Chem. Phys.* **1974**, *60*, 195.
(12) Kohnstamm, Ph. In "Handbuch der Physik"; Geiger, H., Scheel, K., Eds.; Springer: Berlin, 1926; Vol. 10, Chapter 4.
(13) Lang, J. C., Jr.; Widom, B. *Physica A (Amsterdam)* **1975**, *81*, 190.
(14) Šolc, K., unpublished results.
(15) Although the term "three-phase critical point" is more specific, the equivalent (and more common) term "critical end point" shall be used henceforth in this paper.
(16) Note that the term "binodal surface" is used here in somewhat different sense than usual. In ternary systems, it commonly means the surface generated by stacking the binodals for various temperatures on top of each other; i.e., it is a *nonisothermal* surface. For quaternary systems, we use it here for the *isothermal* surface generated by sets of binodals in the complete tetrahedral composition space. The physical definition of the binodal as the locus of two-phase equilibrium compositions is of course preserved in both renditions.